

This discussion paper is/has been under review for the journal Atmospheric Chemistry and Physics (ACP). Please refer to the corresponding final paper in ACP if available.

# Mass-spectrometric identification of primary biological particle markers: indication for low abundance of primary biological material in the pristine submicron aerosol of Amazonia

J. Schneider<sup>1</sup>, F. Freutel<sup>1</sup>, S. R. Zorn<sup>1,2</sup>, Q. Chen<sup>2</sup>, D. K. Farmer<sup>3</sup>, J. L. Jimenez<sup>3</sup>, S. T. Martin<sup>2</sup>, P. Artaxo<sup>4</sup>, A. Wiedensohler<sup>5</sup>, and S. Borrmann<sup>1,6</sup>

<sup>1</sup>Particle Chemistry Department, Max Planck Institute for Chemistry, Mainz, Germany

<sup>2</sup>School of Engineering and Applied Sciences and Department of Earth and Planetary Sciences, Harvard University, Cambridge, MA, USA

<sup>3</sup>Dept. of Chem. & Biochem. & CIRES, University of Colorado, Boulder, CO, USA

<sup>4</sup>Applied Physics Department, Institute of Physics, University of São Paulo, Brazil

<sup>5</sup>Leibniz Institute for Tropospheric Research, Leipzig, Germany

<sup>6</sup>Institute for Atmospheric Physics, Johannes Gutenberg University Mainz, Germany

19143

Received: 31 May 2011 – Accepted: 23 June 2011 – Published: 5 July 2011

Correspondence to: J. Schneider (johannes.schneider@mpic.de)

Published by Copernicus Publications on behalf of the European Geosciences Union.

## Abstract

The abundance of marker compounds for primary biological particles in submicron aerosol was investigated by means of aerosol mass spectrometry. Mass spectra of amino acids, carbohydrates, small peptides, and proteins, all of which are key building blocks of biological particles, were recorded in laboratory experiments. Several characteristic marker peaks were identified. The identified marker peaks were compared with mass spectra recorded during AMAZE-08, a field campaign conducted in the pristine rainforest of the Central Amazon Basin, Brazil, during the wet season of February and March 2008. The low abundance of identified marker peaks places upper limits of 7.5 % for amino acids and 5.6 % for carbohydrates on the contribution of primary biological aerosol particles (PBAPs) to the submicron organic aerosol mass concentration during this time period. Upper limits for the absolute submicron concentrations for both compound classes range from 0.01 to 0.1  $\mu\text{g m}^{-3}$ . Carbohydrates and protein amino acids make up for about two thirds of the dry mass of a biological cell. Thus, our findings suggest an upper limit for the PBAPs mass fraction of about 20 % to the submicron organic aerosol.

## 1 Introduction

Primary biological aerosol particles (PBAPs) are suggested to play an important role in atmospheric aerosol processes and cloud formation (Jaenicke, 2005; Jaenicke et al., 2007; Möhler et al., 2007; Deguillaume et al., 2008; Spracklen et al., 2010). Average number fractions of about 30 % have been reported even in the fine mode aerosol, for aerodynamic particle diameters between 400 nm and 1  $\mu\text{m}$  (Matthias-Maser and Jaenicke, 1995). Primary biological particles in the submicron fraction are expected to be mainly bacteria or viruses, e.g., Hinds (1999). Bacteria are typically rod-shaped, about 1–3  $\mu\text{m}$  long and 0.3–0.5  $\mu\text{m}$  wide (Morris et al., 2004). Size distribution measurements by Möhler et al. (2008) using mobility and aerodynamic particle sizing have

19145

shown that a large fraction of such airborne bacteria is found in the submicron mode. Pollen and fungal spores are generally larger than 1  $\mu\text{m}$  (Jones and Harrison, 2004; Elbert et al., 2007; Huffman et al., 2010), although pollen fragments are also present in the submicron range (Taylor et al., 2002, 2004). The dry mass of a typical bacterial cells contains about 55 % proteins and amino acids, 24 % nucleic acids, 10 % carbohydrates, 7 % lipids, and 5 % inorganic minerals and trace elements (Watson et al., 2007). Mammal cells contain similar amounts of proteins and carbohydrates (68 % and 8 %, respectively), lower amounts of nucleic acids (5 %), but higher amounts of lipids (19 %) (Munk, 2000). The variation found in pollen composition is larger: the dry mass of pollen contains between 10 and 40 % proteins and 13–55 % carbohydrates (Campos et al., 2008). Viruses contain only proteins and nucleic acids (Beyer and Walter, 1988). Since proteins are composed of large chains of amino acids, on average amino acids and carbohydrates contribute about 60 to 80 % of the dry mass of a biological cell.

Although it has been demonstrated in laboratory experiments (Diehl et al., 2001, 2002; von Blohn et al., 2005; Iannone et al., 2011) and field studies (Pratt et al., 2009) that PBAPs can act as efficient ice nuclei (IN), model studies indicate that on a global scale PBAPs account for less than one percent of the global IN fraction, while dust (> 80 %) and soot dominate the IN (Hoose et al., 2010). In regions that are only to a small degree influenced by mineral dust and anthropogenic emissions PBAPs are expected to be of higher importance. One such region is the Amazonian rain forest (Prenni et al., 2009). Another important effect is that PBAP for certain meteorological conditions can take up enough water that they act as “giant” cloud condensation nuclei by generating larger drops that fall faster than drops formed from smaller CCN, thereby facilitating coalescence and warm rain formation (Möhler et al., 2007). They may also limit the potential supersaturation and thus cloud activation of smaller particles by enhanced water depletion. Furthermore, PBAP play a significant role (about 13 %) in the deposition of phosphorus on a global scale (Mahowald et al., 2008; Spracklen et al., 2010). PBAP in Amazonia are reviewed in Martin et al. (2010b).

19146

The Amazonian Aerosol Characterization Experiment 2008 (AMAZE-08) field campaign (Martin et al., 2010a) was conducted in the wet season from February to March 2008. The objective of AMAZE-08 was to improve our understanding of aerosol sources and aerosol-cloud interactions in the pristine Amazonian rain forest. One of the research foci was the assessment of the contribution of PBAPs to the total aerosol, both in number fraction and mass fraction. The ability of PBAPs to act as ice nuclei in the Amazonian rain forest during AMAZE-08 has been shown by Prenni et al. (2009), with observed IN number concentrations of the order of  $1\text{--}2\text{ l}^{-1}$ . Further measurements performed during AMAZE-08 by using the UV-APS technique show that PBAPs are frequently found in the coarse mode (Pöschl et al., 2010). Similar findings have been reported from the Cooperative LBA Airborne Regional Experiment (CLAIRE-2001) experiments (Graham et al., 2003a,b). Nevertheless, it can be possible that the fraction of PBAPs in the fine mode ( $d_{\text{aero}} < 1\ \mu\text{m}$ ) may be more important in the pristine rain-forest of the Central Amazon Basin, which is only slightly influenced by anthropogenic emissions, especially in the wet season.

Laser-ablation single-particle aerosol mass spectrometry has been used in the past to identify PBAP. Czerwieniec et al. (2005) identified fragments of amino acids like glycine, proline, valine, threonine, leucine, isoleucine, histidine, and phenylalanine in positive ion mass spectra from cells and spores of *Bacillus atrophaeus*. Fergenson et al. (2004) detected glutamic acid in negative ion mass spectra of *Bacillus atrophaeus* and *Bacillus thuringiensis*. Furthermore, phosphorus was identified in negative ion mass spectra, suggesting its use as a well-suited marker for bioaerosol because phosphate occur in endospore nucleic acids, adenosine di- and triphosphates, and cell membranes (Fergenson et al., 2004). Russell et al. (2004) studied the behavior of small peptides composed of glycine, arginine, and tyrosine and were able to explain the observed peaks by fragmentation of the amino acid molecules. Another widely used type of aerosol mass spectrometers (Aerodyne Aerosol Mass Spectrometer, AMS) (Canagaratna et al., 2007) is based on thermal desorption and electron ionization (EI), but so far it has not been applied systematically to biological material. Although electron

19147

ionization produces different fragmentation patterns than laser ablation, there are still many similarities in the spectra of organic species from both techniques (Silva and Prather, 2000). Identification of amino acids and amino acid fragments from peptides has been demonstrated using EI (Spiteller, 1966, and references therein). Thus, we expect to be able to identify marker peaks from laboratory measurements of amino acids and to apply those markers to ambient aerosol data. Yttri et al. (2007) demonstrated that sugars, including fructose, glucose, sucrose, and trehalose, as well as sugar alcohols, such as arabitol, inositol, and mannitol, may represent important constituents of the water-soluble organic carbon fraction in the ambient aerosol and can be useful as tracers for PBAP. Therefore, we also investigated carbohydrates as possible marker peaks for PBAPs.

The investigation herein focuses on in-situ measurements of organic aerosol using an Aerodyne Aerosol Mass Spectrometer (AMS) in Amazonia during AMAZE-08 and on the comparison of these field data to the laboratory observations with respect to compounds that are major constituents of PBAP. In the laboratory, mass spectra of particles produced from a selection of amino acids, carbohydrates (sugars), peptides, and proteins were recorded, and marker peaks for PBAP were identified. A comparison of these marker peaks was made to the mass spectra collected for the submicron organic aerosol of AMAZE-08 to assess the relative contribution of PBAPs to the total submicron aerosol.

## 2 Measurements

### 2.1 Experimental identification of marker peaks in laboratory measurements

The laboratory measurements were performed at the Max Planck Institute for Chemistry (MPIC), Mainz (Freutel, 2009). Typical constituents found in biological cells (amino acids, peptides, proteins, and carbohydrates) were analyzed by aerosol mass spectrometry. The compounds were individually dissolved in demineralized water and

19148

nebulized with an atomizer (TSI 3075). The particles were dried by diffusion, size selected by a Differential Mobility Analyzer (DMA; Grimm 5.5–900 or TSI 3080), and introduced into a time-of-flight aerosol mass spectrometer (Aerodyne Inc., compact C-ToF-AMS, Drewnick et al., 2005; or high-resolution HR-ToF-AMS, DeCarlo et al., 2006).  
5 Both instruments operate with thermal desorption at 600 °C and electron impact ionization. They differ only by the type of mass spectrometer: The HR-ToF-AMS provides a higher mass resolving power  $m/\Delta m$  (in “V-mode” typically 2000 at  $m/z$  100 compared to the C-ToF-AMS that has  $m/\Delta m$  of about 800 at  $m/z$  100 (DeCarlo et al., 2006)). While most compounds were measured using the C-ToF-AMS, the HR-ToF-AMS was  
10 used for the measurements of glutathion and levoglucosan.

A list of investigated amino acids is provided in Table 1. From the 20 proteinogenic amino acids (Beyer and Walter, 1988; Munk, 2000), we selected glycine as the simplest amino acid, three amino acids (alanine, valine, leucine) with aliphatic side chains as another important category of compounds, as well as other compounds representing  
15 additional classes: one sulfur-containing amino acid (cysteine), one with an aliphatic side chain and a second carboxyl group (glutamic acid), one aromatic amino acid (tryptophane), and proline, whose amino group is part of cyclo-aliphatic ring. Glutathione, a tripeptide composed of glutamic acid, cysteine, and glycine, was used as an example of a small peptide. In addition to the compounds listed in Table 1, insulin (51  
20 amino acids, molecular weight  $MW \approx 4700 \text{ g mol}^{-1}$ ) and casein (169–209 amino acids,  $MW \approx 19\,000\text{--}25\,000 \text{ g mol}^{-1}$ ) were selected as examples for proteins.

The five carbohydrates that were investigated are listed in Table 2. We selected a monosaccharide (glucose), a disaccharide (saccharose, composed of glucose and fructose), and a polysaccharide (glycogen) composed of up to 50 000 glucose units.  
25 As an example, we selected mannitol as a sugar alcohol, which is a component of fungal spores (Elbert et al., 2007). Levoglucosan, an anhydride of glucose, was also investigated. Levoglucosan is a pyrolysis product of cellulose and is a commonly used tracer for biomass burning aerosol (Simoneit et al., 1999; Fraser and Lakshmanan, 2000).

19149

For each experiment, a blank gas phase measurement using a particle filter was recorded. This blank spectrum was later subtracted from the recorded mass spectrum of the each compound to remove signals originating from the gas phase. This method  
5 avoids any uncertainties that can arise from ion fragmentation and attribution of these fragments to the various components of the gas phase and the particle phase, as is usually done by applying a fragmentation table (Allan et al., 2004) in the standard AMS analysis software (SQUIRREL v1.49, PIKA v1.08, see [http://cires.colorado.edu/jimenez-group/wiki/index.php/ToF-AMS\\_Analysis\\_Software](http://cires.colorado.edu/jimenez-group/wiki/index.php/ToF-AMS_Analysis_Software) and DeCarlo et al., 2006). The mass spectra represent averages over several minutes, corresponding to a number  
10 of sampled particles in the order of  $10^5$ .

## 2.2 Field measurements during AMAZE-08

The field measurements were performed between 7 February and 14 March 2008 during AMAZE-08 (Martin et al., 2010a). The principal measurement site of AMAZE-08 was tower TT34 (2°35.675' S, 60°12.557' W, 110 m a.s.l.). It was located in the Central  
15 Amazon Basin, 60 km NNW of downtown Manaus and 40 km from the metropolis margins. The aerosol was sampled through an inlet with a 7.7  $\mu\text{m}$  cut-off at the top of the tower at a height of 38 m. The sample line was designed to provide laminar flow conditions and the temperature of the flow was kept at 32 °C down to the container to avoid condensation in the pipe below the canopy. On top of the measurement container,  
20 the sampled air was dried to 30–40 % relative humidity using an automatic regenerative dryer (Tuch et al., 2009) and then distributed to various instruments inside of the air-conditioned container.

The ambient data reported here were recorded with an Aerodyne HR-ToF-AMS that was operated in V-mode (DeCarlo et al., 2006). It was equipped with the first prototype  
25 of a high pressure inlet lens designed to transmit larger particles compared to the standard aerodynamic lens of the AMS, which has a 50 % cut off at 640 nm  $d_{va}$  (vacuum aerodynamic diameter) as reported by Liu et al. (2007). Characterization measurements of the prototype showed that this design was only partly successful, since the

19150

50 % cut-off at about 800 nm  $d_{va}$  was only slightly larger than that of the standard lens.

Comparative measurements with a co-located HR-ToF-AMS (operated by Harvard) (Chen et al., 2009) show that the data recorded by both instruments agreed to about 10 % in the overlap region (Fig. 1, after Pöschl et al., 2010). The high pressure lens had slightly more transmission at larger particle diameters ( $> 500$  nm  $d_{va}$ ) but a lower transmission for particles smaller than 260 nm  $d_{va}$ . This difference led to a lower reported total submicron aerosol mass by the MPIC instrument compared to the Harvard instrument because a higher fraction of aerosol mass resided between 100–300 nm than between 500–1000 nm. The objective of the measurements using the high pressure inlet system was to detect primary biological material that is usually expected to be found at larger particle sizes. Thus, for the present analysis the lower transmission for smaller particles is not an issue. The (slightly) higher transmission for larger particles increases the probability to detect PBAP.

The AMS data were analyzed using the standard AMS analysis software (SQUIRREL v1.49, PIKA v1.08). Specific details of the data evaluation are listed in the Supplement.

In order to evaluate the high-resolution mass spectra that are needed to identify the exact marker peaks, the mass spectra were averaged over 12 h (06:00–18:00 and 18:00–06:00 LT). The cumulative peaks were fitted by a selection of exact  $m/z$  that contribute most likely to the cumulative peak, including the respective marker peak. Thus, the relative contribution of the respective marker peak to the respective cumulative peak was inferred. The fraction of only this portion of the cumulative peak to the total organic aerosol signal was then calculated. In this way, the mass fraction of the marker peaks to the total organic aerosol was calculated with 12 h time resolution. Using the laboratory results, these data can be converted into upper limits for the mass concentrations of amino acids and carbohydrates.

19151

### 3 Results

#### 3.1 Identified marker peaks

##### 3.1.1 Amino acids and glutathione

The mass spectra of the examined amino acids and of the tripeptide glutathione (Table 1) are displayed in Fig. 2. The observed peaks can be explained by fragmentation of molecular sub-structures. The most important fragmentation mechanism is the neutral loss of the COOH group (nominal  $m/z$  45, exact  $m/z$  44.997), leading to a dominant peak at  $m/z = M - 45$ , where  $M$  is the molar mass of the original molecule.

Glycine, as the simplest amino acid ( $C_2H_5NO_2$ ), shows a very clear fragmentation pattern. The carboxyl group COOH is lost from the molecule or molecular ion, leading to the  $CH_4N^+$  ion at  $m/z$  30. The molecular ion peak ( $m/z$  75) is also visible. Additional observed ions are  $CO_2^+$ , as is typical of carboxylic acid detection in the AMS (e.g., Duplissy et al., 2011) and  $H_2O^+$  ( $m/z$  44 and 18). The  $H_2O^+$  ion can originate from decomposition of the molecules itself but also from molecular water present in the particles due to incomplete drying.

For alanine ( $MW = 89.10 \text{ g mol}^{-1}$ ), the loss of the COOH group mainly leads to  $C_2H_6N^+$ . This fragment has the same nominal mass to charge ratio as  $CO_2^+$ , namely  $m/z$  44. Additionally, a pronounced peak at  $m/z$  42 ( $C_2H_4N^+$ ) is also observed. Valine and leucine, the other two aliphatic amino acids, have more complex mass spectra, with peaks at  $M$ -COOH ( $m/z$  72 and 86, respectively) and  $M$ -COOH- $CH_4$  ( $m/z$  56 and 70). The mass spectra of both compounds also show a peak at  $m/z$  74 ( $CHNH_2COOH^+$ ), which results from the loss of the aliphatic side chain. The peaks at  $m/z$  39, 41, and 43 can be explained by the loss of  $CHNH_2$  and  $C_2H_3NH_2$  from the  $M$ -COOH peaks at  $m/z$  72 and 86, forming  $C_3H_7^+$  ( $m/z$  43),  $C_3H_3^+$  ( $m/z$  39) and  $C_3H_5^+$  ( $m/z$  41). Other pronounced ions are  $CH_4N^+$  ( $m/z$  30) and  $C_2H_4N^+$  ( $m/z$  42). Similar fragments ( $M$ -COOH,  $CH_4N^+$ ,  $C_2H_4N^+$ , and  $CHNH_2COOH^+$ ) are observed in the mass spectrum of glutamic acid, with additional peaks at  $m/z$  56 ( $C_3H_6N^+$ ) and  $m/z$  84 ( $M$ - $H_2O$ -COOH).

19152

The amino group in the proline molecule is part of an aliphatic ring, leading to a stable ion with  $m/z$  70 ( $C_4H_8N^+$ ) after loss of the COOH group. Further pronounced peaks are found at  $m/z$  41 ( $C_3H_5^+$  or  $C_2H_3N^+$ , not resolved by the C-ToF-AMS),  $m/z$  42 ( $C_2H_4N^+$ ), and  $m/z$  30 ( $CH_4N^+$ ).

5 Tryptophane, as an example for an amino acid with an aromatic side chain, shows a different fragmentation pattern. Here, rather than  $M$ -COOH giving the most prominent peak (at high  $m/z$ ),  $M$ -COOH- $CH_2NH$  forms as a very stable ion at  $m/z$  130 ( $C_9H_8N^+$ , see Fig. 2h). Further fragmentation of this double ring forms the phenyl ion ( $C_6H_5^+$ ,  $m/z$  77) or the styrene-like cation ( $C_8H_7^+$ ,  $m/z$  103). Additional large peaks  
10 at  $m/z$  18 ( $H_2O^+$ ) and  $m/z$  44 ( $CO_2^+$ ) are observed, while the signals at  $m/z$  30 ( $CH_4N^+$ ) and  $m/z$  42 ( $C_2H_4N^+$ ) are small. Cysteine, a sulfur-containing amino acid, has peaks  $M$ -COOH ( $m/z$  76) and  $CHNH_2COOH^+$  ( $m/z$  74). Additionally, sulfur-containing peaks (e.g.,  $C_2HS^+$ ,  $m/z$  57;  $C_2H_3S^+$ ,  $m/z$  59) can be found (Fig. 2e), as well as the peaks at  $m/z$  30 and  $m/z$  42 that have been observed in the mass spectra of the other amino  
15 acids (see above).

The most frequently detected peak  $M$ -COOH is not suitable as a general marker peak of amino acids because it is at a different  $m/z$  for each individual amino acid. The frequently occurring peak at  $m/z$  74, though possibly suitable for the identification of single amino acids, is not applicable to oligomeric peptides and proteins because after  
20 the formation of a peptide bond the  $m/z$  74 fragment is not to be expected any more. The nitrogen containing fragments  $CH_4N^+$  ( $m/z$  30.0344) and  $C_2H_4N^+$  ( $m/z$  42.0344) are the most common characteristic marker peaks.  $CH_4N^+$  was also found to be a characteristic peak in the mass spectra of peptides and amino acids, as obtained by laser ablation mass spectrometry (Russell et al., 2004). The fragment  $m/z$  56 ( $C_3H_6N^+$ ) has  
25 been observed only for larger amino acids and is therefore not well suited as a general marker for amino acids. The fraction of the marker peaks  $CH_4N^+$  and  $C_2H_4N^+$  to the total mass spectrum of each of the examined amino acids is shown in Fig. 3. This fraction was found to be approximately constant ( $0.085 \pm 0.020$ ) for most of the investigated molecules. The inverse of this fraction is used in the present study as a scaling

19153

factor  $SF_{\text{amino}}$ . Glycine and tryptophane were not included in this average. For glycine, the loss of the COOH group yields the  $CH_4N^+$  ion. The fraction of  $m/z$  30 is thus much higher for glycine than for other amino acids. Tryptophane is an aromatic amino acid with stable ring structures, inhibiting further fragmentation. Therefore, the fraction of  
5 these marker peaks is significantly lower than for the other investigated amino acids.

As an example for a small peptide, an oligomer of a limited number of amino acids, glutathione (a tripeptide consisting of glutamic acid, cysteine, and glycine) was analyzed (Fig. 2i). The most prominent peaks are  $m/z$  84 ( $C_4H_6NO^+$ ), which is formed by loss of the glutamic acid side chain and a COOH group, leading to a stable ring structure;  $m/z$  76 ( $C_2H_6NS^+$ , the  $M$ -COOH fragment of cysteine),  $m/z$  56 ( $C_3H_6N^+$ ),  $m/z$  18,  
10 and  $m/z$  44. The above identified marker peaks  $m/z$  30 and 42 are also found in the glutathione spectrum, with a similar fraction as for most investigated amino acids.

### 3.1.2 Proteins

The mass spectra of the two investigated proteins (insulin and casein) are displayed in  
15 Fig. 4. Insulin, which is not soluble in pure water was dissolved in diluted hydrochloric acid. The two corresponding peaks from  $H^{35}Cl^+$  and  $H^{37}Cl^+$  are marked in grey. Insulin, a smaller protein, also shows amino acid fragments that can be identified as  $M$ -COOH. For example,  $m/z$  136 can be identified as the fragment  $M$ -COOH from tyrosine ( $MW = 181 \text{ g mol}^{-1}$ ),  $m/z$  120 from phenylalanine ( $MW = 165 \text{ g mol}^{-1}$ ),  $m/z$  110 from histidine ( $MW = 155 \text{ g mol}^{-1}$ ),  $m/z$  86 from leucine,  $m/z$  72 from valine, and  $m/z$  70 from proline. Tyrosine, phenylalanine, and histidine are aromatic amino acids and thus their fragments  $M$ -COOH are expected to be very stable. Furthermore, the nitrogen-containing peaks that were also identified in many amino acid mass spectra ( $m/z$  56,  $C_3H_6N^+$ ;  $m/z$  42,  $C_2H_4N^+$ ; and  $m/z$  30,  $CH_4N^+$ ) can be detected, although in a smaller  
20 fraction of the total organic mass spectrum (about 0.03) compared to the pure amino acids.  
25

The mass spectrum of casein, a larger protein with a molar mass in the range of  $19\,000$ – $25\,000 \text{ g mol}^{-1}$  is dominated by a large  $CO_2^+$  peak at  $m/z$  44. A sodium

19154

hydroxide solution was added to dissolve the casein in water, which may increase the amount of  $\text{CO}_2^+$  measured via formation of sodium carbonate. However, this pathway was corrected for in a blank measurement of a pure sodium hydroxide solution. Thus, the high peak at  $m/z$  44 may indicate strong thermal decomposition of the molecule and possibly also oxidation of the fragments in the vaporization process of the mass spectrometer. Apart from this dominant peak at  $m/z$  44, some less intense peaks were identified that were also detected in the amino acid mass spectra or in the mass spectrum of insulin. For example, the peak at  $m/z$  70 can be identified as the  $M$ -COOH fragment of proline, which is highly abundant in casein. The peak at  $m/z$  91 ( $\text{C}_7\text{H}_7^+$ ) was also detected in insulin, though not in any of the investigated amino acids. Casein contains only a relatively small amount of aromatic amino acids, and this fact might explain the low number of peaks at higher  $m/z$ , as compared to insulin. Again, the marker peaks  $m/z$  42 and  $m/z$  30 are detected. Their fraction of the total organic signal (without the high  $m/z$  44 peak) is about 0.089, thus very similar to the value found for the pure amino acids of  $0.085 \pm 0.020$  (see above).

Although these results indicate that certain amino acid peaks can be found also in proteins, the complete evaporation of proteins and their full quantification by the use of two amino acid marker peaks still has to be verified.

### 3.1.3 Carbohydrates

Glucose, saccharose, mannitol, levoglucosan, and glycogen were analyzed as examples for carbohydrates and their anhydrides (Table 2). The mass spectra are displayed in Fig. 5. Typical peaks were found for the sequence  $\text{C}_n\text{H}_{2n+1}\text{CO}^+$ , with  $n = 0-2$  ( $\text{CHO}^+$ ,  $m/z$  29;  $\text{C}_2\text{H}_3\text{O}^+$ ,  $m/z$  43;  $\text{C}_3\text{H}_5\text{O}^+$ ,  $m/z$  57), as well as at  $m/z$  44 (with similar contributions by  $\text{CO}_2^+$  and  $\text{C}_2\text{H}_4\text{O}^+$ ). These peaks are commonly found in AMS mass spectra of oxygenated organic compounds, limiting their usefulness as markers for carbohydrates (DeCarlo et al., 2006; Kroll et al., 2009; Sun et al., 2009). Better suited as marker peaks appear to be the ion fragments  $\text{C}_2\text{H}_4\text{O}_2^+$  ( $m/z$  60.0211),  $\text{C}_2\text{H}_5\text{O}_2^+$  ( $m/z$  61.029), and  $\text{C}_3\text{H}_5\text{O}_2^+$  ( $m/z$  73.029). Saccharose and glycogen (the disaccharide and

19155

the polysaccharide) show an important peak at  $m/z$  85 ( $\text{C}_4\text{H}_5\text{O}_2^+$ ), and the sugar alcohol mannitol has a characteristic peak at  $m/z$  56 ( $\text{C}_3\text{H}_4\text{O}^+$ ). The ions at  $m/z$  60 and 73 have been widely used previously as marker peaks for biomass-burning particles (Schneider et al., 2006; Alfara et al., 2007; Lee et al., 2010), mainly because of the release of levoglucosan and related molecules during pyrolysis of cellulose (Simoneit et al., 1999; Fraser and Lakshmanan, 2000). Secondary organic material and fatty acids also fragment at  $m/z$  60 and 73 (Mohr et al., 2009). Thus, for an arbitrary mass spectrum, attribution of these peaks as markers for biomass burning, secondary organic material, or PBA particles cannot be uniquely determined. Nevertheless, the values inferred herein for the ambient spectra can be regarded as upper limits for PBAP carbohydrates.

To obtain a scaling factor for the quantification, we used only glucose, saccharose, and mannitol because levoglucosan is a primary tracer for biomass burning (see above). The large polymer glycogen was found to be less volatile on the AMS vaporizer than the mono- and disaccharides. The mean fraction of the common marker peaks ( $m/z$  60,  $m/z$  61, and  $m/z$  73) to the total mass spectrum of these three compounds was  $0.085 \pm 0.034$  (mean and standard deviation). The inverse of this fraction is used in Sect. 3.2 as a scaling factor  $SF_{\text{carbohydrate}}$ .

## 3.2 Results from the AMAZE-08 field campaign

The time series of non-refractory submicron particle mass concentrations measured with the MPIC HR-ToF-AMS during the AMAZE-08 campaign is shown in Fig. 6. Approximately 72 % of the detected non-refractory submicron particle mass was composed of organic matter, while about 26 % was composed of ammonium and sulfate. Nitrate and chloride were found to be negligible. Slight differences to the values reported by Chen et al. (2009) from the co-located HR-ToF-AMS (Harvard) during AMAZE-08 can be explained by the different inlet transmission functions of the two mass spectrometers. These values are similar to the chemical composition of the fine mode ( $d_{\text{aero}} < 2 \mu\text{m}$ ) of CLAIRE-2001, an earlier campaign in the Amazon Basin. In

19156

CLAIRE-2001, 81 % organics and 16 % sulfate were reported for the non-refractory species mass concentrations by mass, excluding black carbon and soil dust (Graham et al., 2003a). A detailed analysis of the organic fraction measured during AMAZE-08 with the co-located AMS in high-resolution mode has been presented by Chen et al. (2009). The results show that local production of biogenic secondary organic aerosol dominated the submicron organic mass concentration during times with low sulfate to organic ratios. During times with a higher sulfate fraction, the influence of air masses arriving from out of the Amazon Basin increased, and the organic fraction was found to be more oxidized.

For the analysis presented here, the mass spectra recorded by the HR-ToF-AMS equipped with the high pressure lens have been averaged over 12 h, from 06:00 to 18:00 LT and from 18:00 to 06:00 LT. Using the PIKA AMS analysis software, the following ion fragments were fitted to the associated peaks:  $m/z$  30:  $\text{NO}^+$ ,  $\text{CH}_2\text{O}^+$ ,  $\text{CH}_4\text{N}^+$ ,  $\text{C}_2\text{H}_6^+$ ;  $m/z$  42:  $\text{C}_2\text{H}_2\text{O}^+$ ,  $\text{C}_2\text{H}_4\text{N}^+$ ,  $\text{C}_3\text{H}_6^+$ ;  $m/z$  60:  $\text{CSO}^+$ ,  $\text{C}_5^+$ ,  $\text{C}_2\text{H}_4\text{O}_2^+$ ,  $\text{C}_3\text{H}_8\text{O}^+$ ;  $m/z$  61:  $\text{C}_2\text{H}_2\text{Cl}^+$ ,  $\text{C}_5\text{H}^+$ ,  $\text{C}_2\text{H}_5\text{O}_2^+$ ; and  $m/z$  73:  $\text{C}_6\text{H}^+$ ,  $\text{C}_3\text{H}_5\text{O}_2^+$ ,  $\text{C}_3\text{H}_9\text{Si}^+$ ,  $\text{C}_4\text{H}_9\text{O}^+$ . Examples of the peak fitting are shown in Fig. 7.

From these fits, the contributions of the individual marker peaks to the total peak signal at the nominal  $m/z$  were inferred (Fig. S1 in the Supplement). The ratios of the marker peak intensities to the total organic signal were then calculated. The upper limits of the fractions of amino acids or carbohydrates of the total organic signal were estimated as follows:

$$\text{fraction} = SF_{\text{class}} \sum_i (f_i - f_i^{\text{background}}) \quad (1)$$

where  $SF_{\text{class}}$  is the scaling factor for the two compound classes (amino acids and carbohydrates; see Fig. 3 and Sect. 3.1),  $i$  denotes the respective  $m/z$  ratio,  $f_i$  is the ratio of the respective marker peak intensity to the total organic signal, and  $f_i^{\text{background}}$  represents other sources of the marker fragments. Such other sources can be biomass burning, which contributes to a significant fraction to  $m/z$  60. In a recent study, Cubison

19157

et al. (2011) observed a background value for  $f_{60}$  of about  $0.003 \pm 0.0006$  for urban areas without biomass burning influence. Additionally, secondary organic aerosol (SOA) may contribute to the marker ions as well. Chamber results showed values for  $f_{60+61+73}$  of 0.004 and for  $f_{30+42}$  of 0.002 for SOA produced by the photooxidation of isoprene, the ozonolysis of  $\alpha$ -pinene, and the ozonolysis of  $\beta$ -caryophyllene, all at low  $\text{NO}_x$  (Chen et al., 2011). However, it is not clear if the same background values can be applied to ambient air in a tropical rain forest. Another possible source for nitrogen-containing organic ions are amines which have been observed by AMS in urban studies (Aiken et al., 2009; Huffman et al., 2009; Sun et al., 2009). According to these studies amines produce the ionic fragments  $\text{C}_3\text{H}_8\text{N}^+$ ,  $m/z$  58 and  $\text{C}_5\text{H}_{12}\text{N}^+$ ,  $m/z$  86, but also further fragmentation to  $\text{CH}_4\text{N}^+$  and  $\text{C}_2\text{H}_4\text{N}^+$  is conceivable. Again, a background value for amines for tropical rain forest is not known. Therefore, in the present study no background subtraction was applied, such that the reported values represent upper limits for the individual compound classes and therefore also for PBAP.

Figure 8 shows the time series of the results. The time trend of the upper limit of the amino acid fraction (Fig. 8a) shows no diel pattern and remains rather constant, with the exception of two pronounced peaks on 28 February and 5 March. On average, the upper limit of the amino acid fraction is  $7.5(\pm 2.3)$  % of the total submicron organic mass concentration.

The upper limit of the carbohydrate fraction (Fig. 8b) at times shows a diel pattern, with higher values during night time, though this pattern is not consistent over the whole time series. However, the relative maximum values are always found during night time. This would agree with Elbert et al. (2007) who report larger concentrations of mannitol due to fungal emissions during night time in Amazonia. The mean and standard deviation for the upper limit of the carbohydrate fraction is  $5.6(\pm 1.1)$  %. Separated into day and night, we obtain a mean daytime value of  $5.3(\pm 1.0)$  % and a mean nighttime value of  $5.7(\pm 1.2)$  %, showing that there is no statistically significant difference between day and night.

19158



The  $f_{60}$  value in the present study is  $0.0024 \pm 0.0042$ . Comparison with the background value for  $f_{60}$  reported by Cubison et al. (2011),  $0.003 \pm 0.0006$ , our value also implies that the fraction of fresh biomass burning aerosol to the submicron organic aerosol is low to negligible, as discussed in Chen et al. (2009).

5 During most of the time, the upper limit fractions of both amino acids and carbohydrates are within the shaded one-sigma standard deviation area of the mean value in Fig. 8. However, the upper panel of Fig. 8 reveals that on 5 March a markedly higher upper limit fraction of amino acids was observed. This increase was not accompanied by an increase of the carbohydrate marker. The high resolution peaks at  $m/z$  30 and 42 are displayed in Fig. S2 in the Supplement, showing that the marker peaks  $\text{CH}_4\text{N}^+$  and  $\text{C}_2\text{H}_4\text{N}^+$  are clearly enhanced during this 12 h time period. The UMR mass spectrum did not show significant differences from the mass spectra during the previous or the following time period. This event coincides with heavy rain during the afternoon (around 15:00 LT) of March 5. It may be that the observed increase of amino acid markers is related to increased PBAP emissions triggered by the rain event. However, in this case also an increase of the carbohydrate markers would be expected. Enhanced wash-out of water soluble organic material (like carbohydrates or aged SOA) is unlikely, because the total organic mass concentration did not decrease during the rain event. Thus, the reason for the high fraction of the amino acid marker on this day remains unresolved.

20 The upper limits of the absolute mass concentration of the compounds are shown in the lowest panel of Fig. 8, along with the mass concentration of the total submicron organic matter. Both the upper limit concentrations of amino acids and carbohydrates range from 0.01 to  $0.1 \mu\text{g m}^{-3}$ . The mean values and standard deviations are  $0.029 \pm 0.021 \mu\text{g m}^{-3}$  and  $0.022 \pm 0.016 \mu\text{g m}^{-3}$  for amino acids and carbohydrates, respectively. The fine mode concentrations of sugars, sugar alcohols, and anhydro-sugars (including levoglucosan) measured during CLAIRE-2001 ( $\sim 0.07 \mu\text{g m}^{-3}$ ) are of the same order of magnitude though slightly higher (Graham et al., 2003b). The explanation may be that Graham et al. analyzed  $\text{PM}_{2.5}$  and therefore observed higher concentrations. Amino acids and proteins were not analyzed during CLAIRE-2001.

19159

#### 4 Summary and conclusions

In laboratory studies, we identified a set of distinct marker peaks for amino acids and for carbohydrates as marker compounds for primary biological aerosol particles. Marker peaks found for amino acids were  $\text{CH}_4\text{N}^+$  ( $m/z$  30) and  $\text{C}_2\text{H}_4\text{N}^+$  ( $m/z$  42) and for carbohydrates were  $\text{C}_2\text{H}_4\text{O}_2^+$  ( $m/z$  60),  $\text{C}_2\text{H}_5\text{O}^+$  ( $m/z$  61), and  $\text{C}_3\text{H}_5\text{O}_2^+$  ( $m/z$  73). Evaluation of these marker peaks in ambient data allowed for quantitative determination of upper limits for the concentration of these compounds. For carbohydrates, a caution is that carbohydrate anhydrides may also originate in part from biomass burning, especially levoglucosan, though for AMAZE-08 in particular these sources could be ruled out. Some of the marker ions, such as  $m/z$  60 and 73, may also have contributions from other species, such as secondary organic material. Also for the amino acid markers, it cannot be ruled out that other compounds contribute to the marker peaks. Based on these considerations, our results for AMAZE-08 indicate that the upper limit fractional contribution to the total submicron organic aerosol mass concentration was approximately 7.5 % for amino acids and 5.6 % for carbohydrates. Because amino acids in the form of proteins and carbohydrates together account for about 2/3 of a biological cell (Munk, 2000), we can conclude that the upper limit of the total contribution of PBAPs to the submicron organic mass concentration was no more than 20 %. Furthermore, we can say that the contribution of fresh biomass burning was also low, as was already discussed by (Chen et al., 2009). The upper limit for the absolute mass concentration of amino acids was  $0.029 \pm 0.021 \mu\text{g m}^{-3}$ , for carbohydrates it was  $0.022 \pm 0.016 \mu\text{g m}^{-3}$ .

Overall, our results are in agreement with findings reported from other studies during AMAZE-08, which concluded that the submicron organic aerosol is mainly of secondary origin and that PBAPs are mostly found in the coarse mode (Chen et al., 2009; Pöschl et al., 2010), as well as with earlier field campaigns (Martin et al., 2010a). The upper limit sugar content of about 5.6 % is in agreement with fine mode filter data reported by Graham et al. (2003d) in the Amazonian rain forest during CLAIRE-2001. The results from CLAIRE-2001 also showed that PBAPs are mainly found in the coarse mode

19160

and that the organic aerosol which contributed about 70 % to the fine mode aerosol is mainly originating from secondary organic aerosol formation (Graham et al., 2003b; Martin et al., 2010a). A study by Yttri et al. (2007), conducted in urban, suburban and rural sites in Norway, reported that the sum of sugars and sugar-alcohols contributed only 0.2 % to 1.0 % by mass to the PM<sub>2.5</sub> organic carbon fraction.

In previous studies average number fractions of PBAPs of about 30 % in the sub-micron size range have been reported (Matthias-Maser and Jaenicke, 1995; Jaenicke et al., 2007). It is expected that PBAPs are mostly found in the upper size range of the submicron aerosol. Airborne bacteria are in the size range around 700 nm (Möhler et al., 2007). Thus, a number fraction of 30 % would imply a mass fraction much higher than 20 %. Taking into account the results of this study as well as the results from Graham et al. (2003a,b) and Yttri et al. (2007), which all at least for the sugars and sugar alcohols show very little contribution to the total organic mass in PM<sub>2.5</sub>, it can be concluded that such high number fractions of up to 30 % in the submicron size range may be found occasionally but are not representative.

**Supplementary material related to this article is available online at:  
[http://www.atmos-chem-phys-discuss.net/11/19143/2011/  
acpd-11-19143-2011-supplement.pdf](http://www.atmos-chem-phys-discuss.net/11/19143/2011/acpd-11-19143-2011-supplement.pdf)**

*Acknowledgement.* We would like to thank the complete AMAZE-08 team, but especially H. Haudeck, T. Böttger, and M. Brands. We also thank F. Drewnick for providing the HR-ToF-AMS and discussion on data evaluation and interpretation. Support by the LBA project and INPA (Manaus) is acknowledged. This work was funded by the Max Planck Society. SRZ was funded by the DFG Graduiertenkolleg GRK826. The USA National Science Foundation (ATM-0723582; ATM-0919189) supported QC, DKF, JLJ, and STM.

The service charges for this open access publication have been covered by the Max Planck Society.

19161

## References

- Aiken, A. C., Salcedo, D., Cubison, M. J., Huffman, J. A., DeCarlo, P. F., Ulbrich, I. M., Docherty, K. S., Sueper, D., Kimmel, J. R., Worsnop, D. R., Trimborn, A., Northway, M., Stone, E. A., Schauer, J. J., Volkamer, R. M., Fortner, E., de Foy, B., Wang, J., Laskin, A., Shutthanandan, V., Zheng, J., Zhang, R., Gaffney, J., Marley, N. A., Paredes-Miranda, G., Arnott, W. P., Molina, L. T., Sosa, G., and Jimenez, J. L.: Mexico City aerosol analysis during MILAGRO using high resolution aerosol mass spectrometry at the urban supersite (T0) – Part 1: Fine particle composition and organic source apportionment, *Atmos. Chem. Phys.*, 9, 6633–6653, doi:10.5194/acp-9-6633-2009, 2009.
- Alfarra, M. R., Prevot, A. S. H., Szidat, S., Sandradewi, J., Weimer, S., Lanz, V. A., Schreiber, D., Mohr, M., and Baltensperger, U.: Identification of the mass spectral signature of organic aerosols from wood burning emissions, *Environ. Sci. Technol.*, 41, 5770–5777, doi:10.1021/es062289b, 2007.
- Allan, J. D., Jimenez, J. L., Williams, P. I., Alfarra, M. R., Bower, K. N., Jayne, J. T., Coe, H., and Worsnop, D. R.: Quantitative sampling using an Aerodyne aerosol mass spectrometer – 1. Techniques of data interpretation and error analysis, *J. Geophys. Res.-Atmos.*, 108, 4090, 2003.
- Allan, J. D., Delia, A. E., Coe, H., Bower, K. N., Alfarra, M. R., Jimenez, J. L., Middlebrook, A. M., Drewnick, F., Onasch, T. B., Canagaratna, M. R., Jayne, J. T., and Worsnop, D. R.: A generalised method for the extraction of chemically resolved mass spectra from aerodyne aerosol mass spectrometer data, *J. Aerosol. Sci.*, 35, 909–922, 2004.
- Beyer, H. and Walter, W.: *Lehrbuch der organischen Chemie*, Hirzel, Stuttgart, 1988.
- von Blohn, N., Mitra, S. K., Diehl, K., and Borrmann, S.: The ice nucleating ability of pollen: Part III: New laboratory studies in immersion and contact freezing modes including more pollen types, *Atmos. Res.*, 78, 182–189, doi:10.1016/j.atmosres.2005.03.008, 2005.
- Campos, M. G. R., Bogdanov, S., de Almeida-Muradian, L. B., Szczesna, T., Mancebo, Y., Frigerio, C., and Ferreira, F.: Pollen composition and standardisation of analytical methods, *J. Apicult. Res.*, 47, 154–161, 2008.
- Canagaratna, M. R., Jayne, J. T., Jimenez, J. L., Allan, J. D., Alfarra, M. R., Zhang, Q., Onasch, T. B., Drewnick, F., Coe, H., Middlebrook, A., Delia, A., Williams, L. R., Trimborn, A. M., Northway, M. J., DeCarlo, P. F., Kolb, C. E., Davidovits, P., and Worsnop, D. R.: Chemical and microphysical characterization of ambient aerosols with the aerodyne aerosol

19162

- mass spectrometer, *Mass Spectrom. Rev.*, 26, 185–222, 2007.
- Chen, Q., Farmer, D. K., Schneider, J., Zorn, S. R., Heald, C. L., Karl, T. G., Guenther, A., Allan, J. D., Robinson, N., Coe, H., Kimmel, J. R., Pauliquevis, T., Borrmann, S., Poschl, U., Andreae, M. O., Artaxo, P., Jimenez, J. L., and Martin, S. T.: Mass spectral characterization of submicron biogenic organic particles in the Amazon Basin, *Geophys. Res. Lett.*, 36, L20806, doi:10.1029/2009gl039880, 2009.
- Cubison, M. J., Ortega, A. M., Hayes, P. L., Farmer, D. K., Day, D., Lechner, M. J., Brune, W. H., Apel, E., Diskin, G. S., Fisher, J. A., Fuelberg, H. E., Hecobian, A., Knapp, D. J., Mikoviny, T., Riemer, D., Sachse, G. W., Sessions, W., Weber, R. J., Weinheimer, A. J., Wisthaler, A., and Jimenez, J. L.: Effects of aging on organic aerosol from open biomass burning smoke in aircraft and lab studies, *Atmos. Chem. Phys. Discuss.*, 11, 12103–12140, doi:10.5194/acpd-11-12103-2011, 2011.
- Czerwieniec, G. A., Russell, S. C., Tobias, H. J., Pitesky, M. E., Fergenson, D. P., Steele, P., Srivastava, A., Horn, J. M., Frank, M., Gard, E. E., and Lebrilla, C. B.: Stable isotope labeling of entire *Bacillus atrophaeus* spores and vegetative cells using bioaerosol mass spectrometry, *Anal. Chem.*, 77, 1081–1087, doi:10.1021/AC0488098, 2005.
- DeCarlo, P. F., Kimmel, J. R., Trimborn, A., Northway, M. J., Jayne, J. T., Aiken, A. C., Gonin, M., Fuhrer, K., Horvath, T., Docherty, K. S., Worsnop, D. R., and Jimenez, J. L.: Field-deployable, high-resolution, time-of-flight aerosol mass spectrometer, *Anal. Chem.*, 78, 8281–8289, 2006.
- Deguillaume, L., Leriche, M., Amato, P., Ariya, P. A., Delort, A.-M., Pöschl, U., Chaumerliac, N., Bauer, H., Flossmann, A. I., and Morris, C. E.: Microbiology and atmospheric processes: chemical interactions of primary biological aerosols, *Biogeosciences*, 5, 1073–1084, doi:10.5194/bg-5-1073-2008, 2008.
- Diehl, K., Quick, C., Matthias-Maser, S., Mitra, S. K., and Jaenicke, R.: The ice nucleating ability of pollen – Part I: Laboratory studies in deposition and condensation freezing modes, *Atmos. Res.*, 58, 75–87, 2001.
- Diehl, K., Matthias-Maser, S., Jaenicke, R., and Mitra, S. K.: The ice nucleating ability of pollen – Part II: Laboratory studies in immersion and contact freezing modes, *Atmos. Res.*, 61, 125–133, 2002.
- Duplissy, J., DeCarlo, P. F., Dommen, J., Alfarra, M. R., Metzger, A., Barmpadimos, I., Prevot, A. S. H., Weingartner, E., Tritscher, T., Gysel, M., Aiken, A. C., Jimenez, J. L., Canagaratna, M. R., Worsnop, D. R., Collins, D. R., Tomlinson, J., and Baltensperger, U.: Relating

19163

- hygroscopicity and composition of organic aerosol particulate matter, *Atmos. Chem. Phys.*, 11, 1155–1165, doi:10.5194/acp-11-1155-2011, 2011.
- Elbert, W., Taylor, P. E., Andreae, M. O., and Pöschl, U.: Contribution of fungi to primary biogenic aerosols in the atmosphere: wet and dry discharged spores, carbohydrates, and inorganic ions, *Atmos. Chem. Phys.*, 7, 4569–4588, doi:10.5194/acp-7-4569-2007, 2007.
- Fergenson, D. P., Pitesky, M. E., Tobias, H. J., Steele, P. T., Czerwieniec, G. A., Russell, S. C., Lebrilla, C. B., Horn, J. M., Coffee, K. R., Srivastava, A., Pillai, S. P., Shih, M. T. P., Hall, H. L., Ramponi, A. J., Chang, J. T., Langlois, R. G., Estacio, P. L., Hadley, R. T., Frank, M., and Gard, E. E.: Reagentless detection and classification of individual bioaerosol particles in seconds, *Anal. Chem.*, 76, 373–378, doi:10.1021/AC034467e, 2004.
- Fraser, M. P. and Lakshmanan, K.: Using levoglucosan as a molecular marker for the long-range transport of biomass combustion aerosols, *Environ. Sci. Technol.*, 34, 4560–4564, doi:10.1021/es991229l, 2000.
- Freutel, F.: Identifizierung charakteristischer massenspektrometrischer Marker für primäre biologische Aerosolpartikel, M.S. Thesis, University Mainz, 2009.
- Graham, B., Guyon, P., Maenhaut, W., Taylor, P. E., Ebert, M., Matthias-Maser, S., Mayol-Bracero, O. L., Godoi, R. H. M., Artaxo, P., Meixner, F. X., Moura, M. A. L., Rocha, C., Van Grieken, R., Glovsky, M. M., Flagan, R. C., and Andreae, M. O.: Composition and diurnal variability of the natural Amazonian aerosol, *J. Geophys. Res.-Atmos.*, 108, 4765, doi:10.1029/2003jd004049, 2003a.
- Graham, B., Guyon, P., Taylor, P. E., Artaxo, P., Maenhaut, W., Glovsky, M. M., Flagan, R. C., and Andreae, M. O.: Organic compounds present in the natural Amazonian aerosol: characterization by gas chromatography-mass spectrometry, *J. Geophys. Res.-Atmos.*, 108, doi:10.1029/2003jd003990, 2003b.
- Hinds, W. C.: *Aerosol Technology – Properties, Behaviour, and Measurements of Airborne Particles*, 2nd edn., John Wiley & Sons, Inc., New York, 1999.
- Hogrefe, O., Drewnick, F., Lala, G. G., Schwab, J. J., and Demerjian, K. L.: Development, operation and applications of an aerosol generation, calibration and research facility, *Aerosol Sci. Technol.*, 38, 196–214, doi:10.1080/02786820390229516, 2004.
- Hoose, C., Kristjansson, J. E., and Burrows, S. M.: How important is biological ice nucleation in clouds on a global scale?, *Environ. Res. Lett.*, 5, 024009, doi:10.1088/1748-9326/5/2/024009, 2010.
- Huffman, J. A., Docherty, K. S., Aiken, A. C., Cubison, M. J., Ulbrich, I. M., DeCarlo, P. F.,

19164

- Sueper, D., Jayne, J. T., Worsnop, D. R., Ziemann, P. J., and Jimenez, J. L.: Chemically-resolved aerosol volatility measurements from two megacity field studies, *Atmos. Chem. Phys.*, 9, 7161–7182, doi:10.5194/acp-9-7161-2009, 2009.
- Huffman, J. A., Treutlein, B., and Pöschl, U.: Fluorescent biological aerosol particle concentrations and size distributions measured with an Ultraviolet Aerodynamic Particle Sizer (UV-APS) in Central Europe, *Atmos. Chem. Phys.*, 10, 3215–3233, doi:10.5194/acp-10-3215-2010, 2010.
- Iannone, R., Chernoff, D. I., Pringle, A., Martin, S. T., and Bertram, A. K.: The ice nucleation ability of one of the most abundant types of fungal spores found in the atmosphere, *Atmos. Chem. Phys.*, 11, 1191–1201, doi:10.5194/acp-11-1191-2011, 2011.
- Jaenicke, R.: Abundance of cellular material and proteins in the atmosphere, *Science*, 308, 73–73, 2005.
- Jaenicke, R., Matthias-Maser, S., and Gruber, S.: Omnipresence of biological material in the atmosphere, *Environ. Chem.*, 4, 217–220, doi:10.1071/en07021, 2007.
- Jones, A. M. and Harrison, R. M.: The effects of meteorological factors on atmospheric bioaerosol concentrations – a review, *Sci. Total Environ.*, 326, 151–180, doi:10.1016/j.scitotenv.2003.11.021, 2004.
- Kroll, J. H., Smith, J. D., Che, D. L., Kessler, S. H., Worsnop, D. R., and Wilson, K. R.: Measurement of fragmentation and functionalization pathways in the heterogeneous oxidation of oxidized organic aerosol, *Phys. Chem. Chem. Phys.*, 11, 8005–8014, doi:10.1039/B905289e, 2009.
- Lee, T., Sullivan, A. P., Mack, L., Jimenez, J. L., Kreidenweis, S. M., Onasch, T. B., Worsnop, D. R., Malm, W., Wold, C. E., Hao, W. M., and Collett, J. L.: Chemical smoke marker emissions during flaming and smoldering phases of laboratory open burning of wildland fuels, *Aerosol Sci. Technol.*, 44, I–V, doi:10.1080/02786826.2010.499884, 2010.
- Liu, P. S. K., Deng, R., Smith, K. A., Williams, L. R., Jayne, J. T., Canagaratna, M. R., Moore, K., Onasch, T. B., Worsnop, D. R., and Deshler, T.: Transmission efficiency of an aerodynamic focusing lens system: Comparison of model calculations and laboratory measurements for the Aerodyne Aerosol Mass Spectrometer, *Aerosol Sci. Technol.*, 41, 721–733, doi:10.1080/02786820701422278, 2007.
- Mahowald, N., Jickells, T. D., Baker, A. R., Artaxo, P., Benitez-Nelson, C. R., Bergametti, G., Bond, T. C., Chen, Y., Cohen, D. D., Herut, B., Kubilay, N., Losno, R., Luo, C., Maenhaut, W., McGee, K. A., Okin, G. S., Siefert, R. L., and Tsukuda, S.: Global distribution of

19165

- atmospheric phosphorus sources, concentrations and deposition rates, and anthropogenic impacts, *Global Biogeochem. Cy.*, 22, GB4026, doi:10.1029/2008gb003240, 2008.
- Martin, S. T., Andreae, M. O., Althausen, D., Artaxo, P., Baars, H., Borrmann, S., Chen, Q., Farmer, D. K., Guenther, A., Gunthe, S. S., Jimenez, J. L., Karl, T., Longo, K., Manzi, A., Müller, T., Pauliquevis, T., Petters, M. D., Prenni, A. J., Pöschl, U., Rizzo, L. V., Schneider, J., Smith, J. N., Swietlicki, E., Tota, J., Wang, J., Wiedensohler, A., and Zorn, S. R.: An overview of the Amazonian Aerosol Characterization Experiment 2008 (AMAZE-08), *Atmos. Chem. Phys.*, 10, 11415–11438, doi:10.5194/acp-10-11415-2010, 2010.
- Martin, S. T., Andreae, M. O., Artaxo, P., Baumgardner, D., Chen, Q., Goldstein, A. H., Guenther, A., Heald, C. L., Mayol-Bracero, O. L., McMurry, P. H., Pauliquevis, T., Poschl, U., Prather, K. A., Roberts, G. C., Saleska, S. R., Dias, M. A. S., Spracklen, D. V., Swietlicki, E., and Trebs, I.: Sources and properties of Amazonian aerosol particles, *Rev. Geophys.*, 48, Rg2002, doi:10.1029/2008rg000280, 2010b.
- Matthias-Maser, S. and Jaenicke, R.: The size distribution of primary biological aerosol particles with radii  $>0.2\ \mu\text{m}$  in an urban rural influenced region, *Atmos. Res.*, 39, 279–286, 1995.
- Möhler, O., DeMott, P. J., Vali, G., and Levin, Z.: Microbiology and atmospheric processes: the role of biological particles in cloud physics, *Biogeosciences*, 4, 1059–1071, doi:10.5194/bg-4-1059-2007, 2007.
- Möhler, O., Georgakopoulos, D. G., Morris, C. E., Benz, S., Ebert, V., Hunsmann, S., Saathoff, H., Schnaiter, M., and Wagner, R.: Heterogeneous ice nucleation activity of bacteria: new laboratory experiments at simulated cloud conditions, *Biogeosciences*, 5, 1425–1435, doi:10.5194/bg-5-1425-2008, 2008.
- Mohr, C., Huffman, J. A., Cubison, M. J., Aiken, A. C., Docherty, K. S., Kimmel, J. R., Ulbrich, I. M., Hannigan, M., and Jimenez, J. L.: Characterization of primary organic aerosol emissions from meat cooking, trash burning, and motor vehicles with high-resolution aerosol mass spectrometry and comparison with ambient and chamber observations, *Environ. Sci. Technol.*, 43, 2443–2449, doi:10.1021/es8011518, 2009.
- Morris, C. E., Georgakopoulos, D. G., and Sands, D. C.: Ice nucleation active bacteria and their potential role in precipitation, *J. Phys. IV*, 121, 87–103, doi:10.1051/jp4:2004121004, 2004.
- Munk, K.: *Biochemie, Zellbiologie, Ökologie, Evolution*, Spektrum Akademischer Verlag, Heidelberg, 2000.
- Ng, N. L., Canagaratna, M. R., Zhang, Q., Jimenez, J. L., Tian, J., Ulbrich, I. M., Kroll, J. H., Docherty, K. S., Chhabra, P. S., Bahreini, R., Murphy, S. M., Seinfeld, J. H., Hildebrandt, L.,

19166

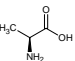
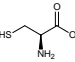
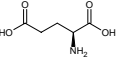
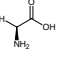
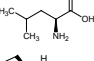
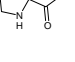
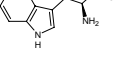
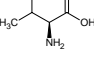
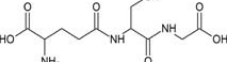
- Donahue, N. M., DeCarlo, P. F., Lanz, V. A., Prévôt, A. S. H., Dinar, E., Rudich, Y., and Worsnop, D. R.: Organic aerosol components observed in Northern Hemispheric datasets from Aerosol Mass Spectrometry, *Atmos. Chem. Phys.*, 10, 4625–4641, doi:10.5194/acp-10-4625-2010, 2010.
- 5 Pöschl, U., Martin, S. T., Sinha, B. W., Chen, Q., Gunthe, S. S., Huffman, J. A., Borrmann, S., Farmer, D., Garland, R. M., Helas, G., Jimenez, J., King, S. M., Manzi, A., Mikhailov, E., Pauliquevis, T., Petters, M. D., Prenni, A. J., Roldin, P., Rose, D., Schneider, J., Su, H., Zorn, S. R., Artaxo, P., and Andreae, M. O.: Rainforest aerosols as biogenic nuclei of clouds and precipitation in the Amazon, *Science*, 1513–1516, 2010.
- 10 Pratt, K. A., DeMott, P. J., French, J. R., Wang, Z., Westphal, D. L., Heymsfield, A. J., Twohy, C. H., Prenni, A. J., and Prather, K. A.: In situ detection of biological particles in cloud ice-crystals, *Nature Geosci.*, 2, 397–400, doi:10.1038/ngeo521, 2009.
- Prenni, A. J., Petters, M. D., Kreidenweis, S. M., Heald, C. L., Martin, S. T., Artaxo, P., Garland, R. M., Wollny, A. G., and Pöschl, U.: Relative roles of biogenic emissions and Saharan dust as ice nuclei in the Amazon Basin, *Nature Geosci.*, 2, 401–404, doi:10.1038/ngeo517, 2009.
- 15 Russell, S. C., Czerwieniec, G., Lebrilla, C., Tobias, H., Fergenson, D. P., Steele, P., Pitesky, M., Horn, J., Srivastava, A., Frank, M., and Gard, E. E.: Toward understanding the ionization of biomarkers from micrometer particles by bio-aerosol mass spectrometry, *J. Am. Soc. Mass Spectrom.*, 15, 900–909, 2004.
- 20 Schneider, J., Weimer, S., Drewnick, F., Borrmann, S., Helas, G., Gwaze, P., Schmid, O., Andreae, M. O., and Kirchner, U.: Mass spectrometric analysis and aerodynamic properties of various types of combustion-related aerosol particles, *Int. Mass J. Spectrom.*, 258, 37–49, 2006.
- 25 Silva, P. J. and Prather, K. A.: Interpretation of mass spectra from organic compounds in aerosol time-of-flight mass spectrometry, *Anal. Chem.*, 72, 3553–3562, 2000.
- Simoneit, B. R. T., Schauer, J. J., Nolte, C. G., Oros, D. R., Elias, V. O., Fraser, M. P., Rogge, W. F., and Cass, G. R.: Levoglucosan, a tracer for cellulose in biomass burning and atmospheric particles, *Atmos. Environ.*, 33, 173–182, 1999.
- 30 Spiteller, G.: *Massenspektrometrische Strukturanalyse organischer Verbindungen*, Verlag Chemie, Weinheim, 1966.
- Spracklen, D. V., Carslaw, K. S., Merikanto, J., Mann, G. W., Reddington, C. L., Pickering, S., Ogren, J. A., Andrews, E., Baltensperger, U., Weingartner, E., Boy, M., Kulmala, M.,

19167

- Laakso, L., Lihavainen, H., Kivekäs, N., Komppula, M., Mihalopoulos, N., Kouvarakis, G., Jennings, S. G., O'Dowd, C., Birmili, W., Wiedensohler, A., Weller, R., Gras, J., Laj, P., Sellegri, K., Bonn, B., Krejci, R., Laaksonen, A., Hamed, A., Minikin, A., Harrison, R. M., Talbot, R., and Sun, J.: Explaining global surface aerosol number concentrations in terms of primary emissions and particle formation, *Atmos. Chem. Phys.*, 10, 4775–4793, doi:10.5194/acp-10-4775-2010, 2010.
- 5 Sun, Y., Zhang, Q., Macdonald, A. M., Hayden, K., Li, S. M., Liggio, J., Liu, P. S. K., Anlauf, K. G., Leaitch, W. R., Steffen, A., Cubison, M., Worsnop, D. R., van Donkelaar, A., and Martin, R. V.: Size-resolved aerosol chemistry on Whistler Mountain, Canada with a high-resolution aerosol mass spectrometer during INTEX-B, *Atmos. Chem. Phys.*, 9, 3095–3111, doi:10.5194/acp-9-3095-2009, 2009.
- 10 Taylor, P. E., Flagan, R. C., Valenta, R., and Glovsky, M. M.: Release of allergens as respirable aerosols: a link between grass pollen and asthma, *J. Allergy Clin. Immunol.*, 109, 51–56, doi:10.1067/mai.2002.120759, 2002.
- 15 Taylor, P. E., Flagan, R. C., Miguel, A. G., Valenta, R., and Glovsky, M. M.: Birch pollen rupture and the release of aerosols of respirable allergens, *Clin. Exp. Allergy*, 34, 1591–1596, doi:10.1111/j.1365-2222.2004.02078.x, 2004.
- Tuch, T. M., Haudek, A., Müller, T., Nowak, A., Wex, H., and Wiedensohler, A.: Design and performance of an automatic regenerating adsorption aerosol dryer for continuous operation at monitoring sites, *Atmos. Meas. Tech.*, 2, 417–422, doi:10.5194/amt-2-417-2009, 2009.
- 20 Watson, J. D., Baker, T. A., Bell, S. P., Gann, A. A. F., Levine, M., and Losick, R. M.: *Molecular biology of the gene*, 6th ed., Benjamin Cummings, 880 pp., 2007.
- Yttri, K. E., Dye, C., and Kiss, G.: Ambient aerosol concentrations of sugars and sugar-alcohols at four different sites in Norway, *Atmos. Chem. Phys.*, 7, 4267–4279, doi:10.5194/acp-7-4267-2007, 2007.
- 25

19168

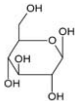
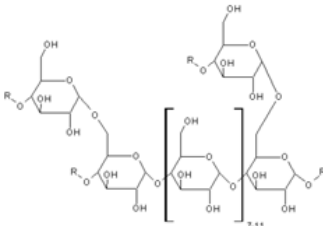
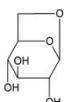
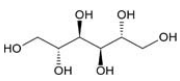
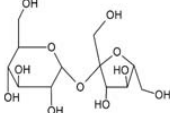
**Table 1.** Amino acids analyzed in the laboratory.

Substance	Formula	Structure	Molecular weight (g mol <sup>-1</sup> )
Alanine <sup>1</sup>	C <sub>3</sub> H <sub>7</sub> NO <sub>2</sub>		89.10
Cysteine <sup>2</sup>	C <sub>3</sub> H <sub>7</sub> NO <sub>2</sub> S		121.16
Glutamic acid <sup>3</sup>	C <sub>5</sub> H <sub>9</sub> NO <sub>4</sub>		147.13
Glycine <sup>4</sup>	C <sub>2</sub> H <sub>5</sub> NO <sub>2</sub>		75.07
Leucine <sup>5</sup>	C <sub>6</sub> H <sub>13</sub> NO <sub>2</sub>		131.18
Proline <sup>1</sup>	C <sub>5</sub> H <sub>9</sub> NO <sub>2</sub>		115.13
Tryptophane <sup>1</sup>	C <sub>11</sub> H <sub>12</sub> N <sub>2</sub> O <sub>2</sub>		204.23
Valine <sup>1</sup>	C <sub>5</sub> H <sub>11</sub> NO <sub>2</sub>		117.15
Glutathion <sup>1</sup> (tripeptide)	C <sub>10</sub> H <sub>17</sub> N <sub>3</sub> O <sub>6</sub>		303.33

Manufacturer: <sup>1</sup> Roth, <sup>2</sup> Sigma Aldrich, <sup>3</sup> Acros Organics, <sup>4</sup> Merck, <sup>5</sup> Fluka;  
Purity: ≥ 97 %.

19169

**Table 2.** Carbohydrates investigated in the laboratory.

Substance	Formula	Structure	Molecular weight (g mol <sup>-1</sup> )
Glucose <sup>1</sup>	C <sub>6</sub> H <sub>12</sub> O <sub>6</sub>		180.06
Glycogen <sup>1</sup>	<(C <sub>6</sub> H <sub>10</sub> O <sub>5</sub> ) <sub>n</sub>		10 <sup>6</sup> –10 <sup>7</sup>
Levoglucozan <sup>2</sup>	C <sub>6</sub> H <sub>10</sub> O <sub>5</sub>		162.05
Mannitol <sup>3</sup>	C <sub>6</sub> H <sub>14</sub> O <sub>6</sub>		182.08
Saccharose <sup>1</sup>	C <sub>12</sub> H <sub>22</sub> O <sub>11</sub>		342.12

Manufacturer: <sup>1</sup> Roth, <sup>2</sup> Fluka, <sup>3</sup> Alfa Aesar.

19170

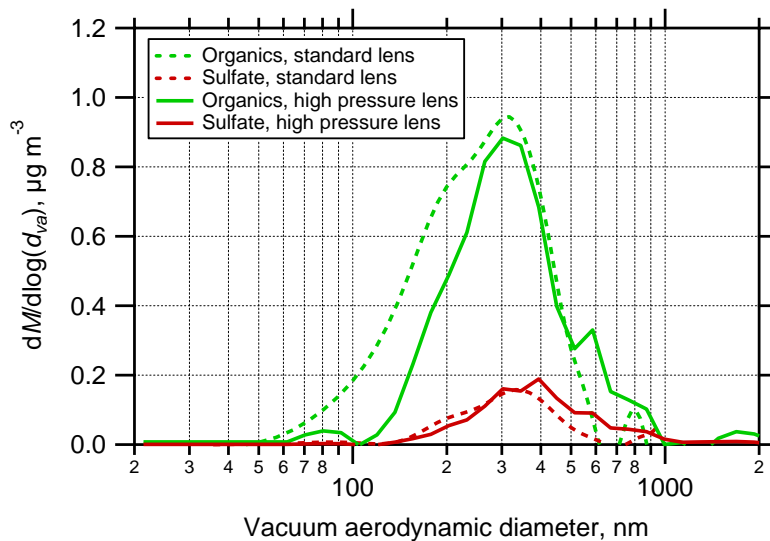


**Fig. 1.** Size distributions measured during AMAZE-08 by the two co-located HR-ToF-AMS instruments (Pöschl et al., 2010). The Harvard AMS used the “standard lens”, the MPIC AMS used a prototype of the “high pressure lens”. The “high pressure lens” provided slightly higher transmission for particle sizes  $> 500$  nm  $d_{va}$ .

19171

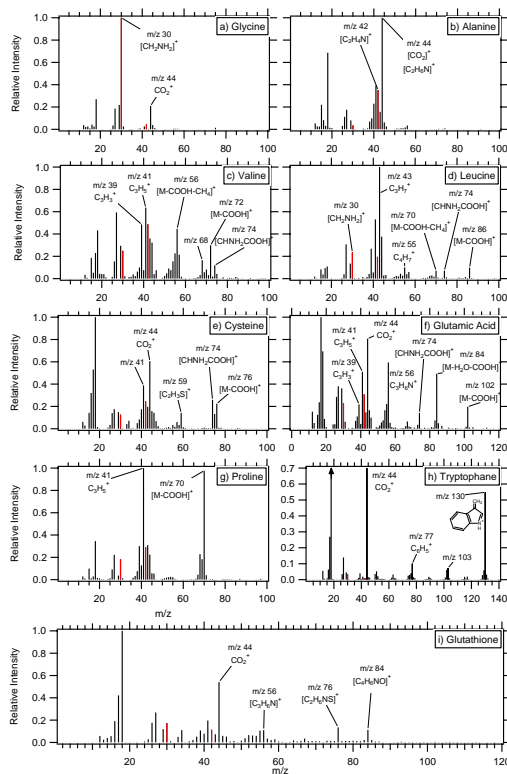


**Fig. 2.** Laboratory mass spectra from amino acid particles. The identified marker peaks ( $m/z$  30 and 42) are highlighted in red. Certain identified peaks are labeled.

19172

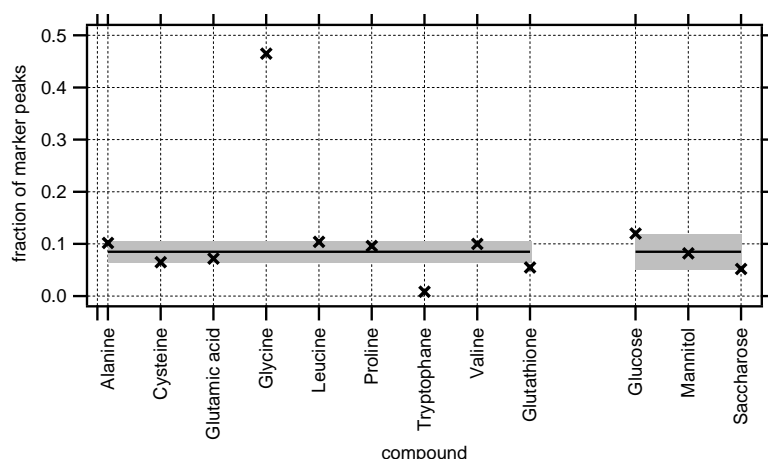


**Fig. 3.** Fraction of marker peaks ( $m/z$  30 and 42 for amino acids and glutathione,  $m/z$  60, 61, and 73 for carbohydrates) in the mass spectra for the investigated amino acids, the tripeptide glutathione and the carbohydrates. Solid line: Mean values (left: amino acids and glutathione without glycine and tryptophane, right: carbohydrates), shaded areas: standard deviation.

19173

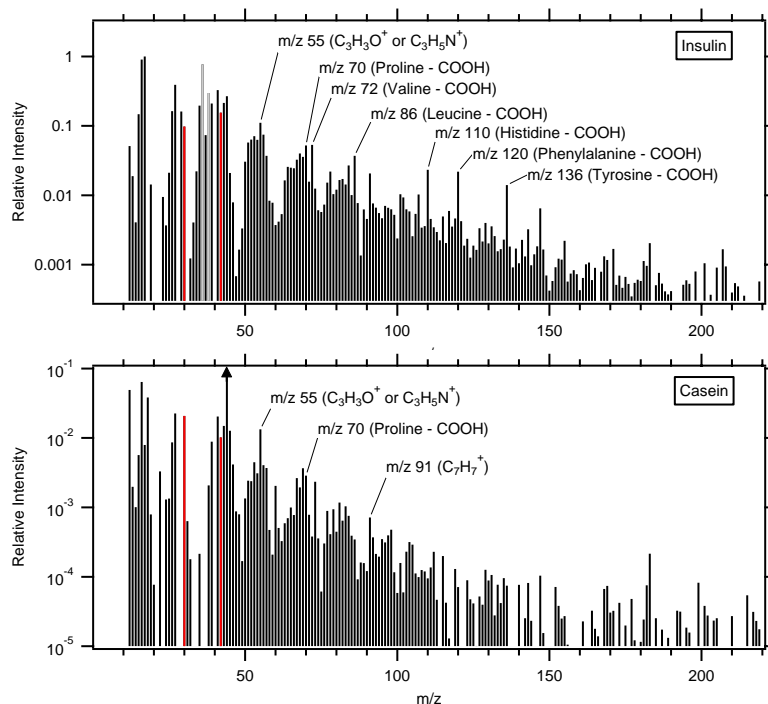


**Fig. 4.** Mass spectra of the two proteins investigated. The identified marker peaks for amino acids ( $m/z$  30 and 42) are highlighted (red). Selected identified peaks are labeled. Insulin was dissolved in HCl, the corresponding peaks ( $m/z$  36 and 38) are marked in grey.

19174



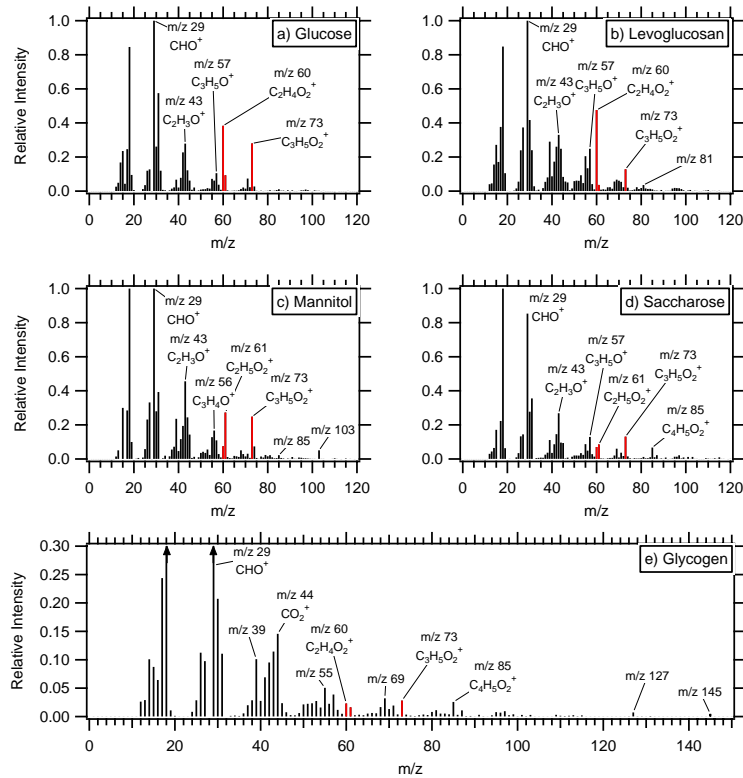


**Fig. 5.** Mass spectra of the carbohydrates investigated in the laboratory. The identified marker peaks ( $m/z$  60, 61, and 73) are highlighted in red.

19175

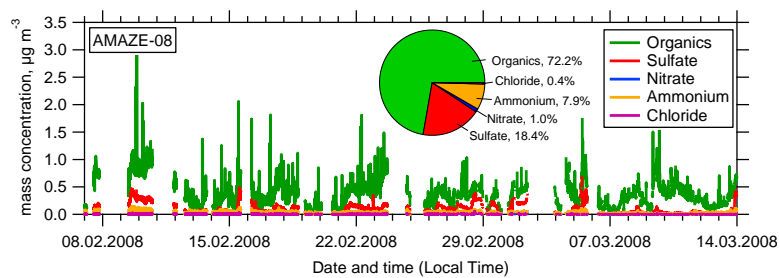


**Fig. 6.** Time series of non-refractory submicron particulate mass concentrations during AMAZE-08 measured by the AMS operating with the high pressure lens. Approximately 72 % of the detected aerosol mass was composed of organic matter, while ammonium sulfate contributed about 26 %. Nitrate and chloride were found to be negligible. Measurement periods that were possibly influenced by local emission sources like vehicle exhaust, the exhaust of the on-site power generator, or regional anthropogenically polluted outflow from Manaus arriving at the sampling tower were excluded (Martin et al., 2010a).

19176

